RADIATION RESEARCH 152, 88–97 (1999)
0033-7587/99 $5.00

RAPID COMMUNICATION

Evidence for Pronounced Bystander Effects Caused by Nonuniform Distributions of Radioactivity using a Novel Three-Dimensional Tissue Culture Model

Anupam Bishayee, Dandamudi V. Rao and Roger W. Howell[1]

Division of Radiation Research, Department of Radiology, New Jersey Medical School, University of Medicine and Dentistry of New Jersey, Newark, New Jersey 07103

Bishayee, A., Rao, D. V. and Howell, R. W. Evidence for Pronounced Bystander Effects Caused by Nonuniform Distributions of Radioactivity using a Novel Three-Dimensional Tissue Culture Model. *Radiat. Res.* 152, 88–97 (1999).

A new *in vitro* multicellular cluster model has been developed to assess the impact of nonuniform distributions of radioactivity on the biological response of mammalian cells, and the relative importance of bystander effects compared to conventional radiation effects. Chinese hamster V79 cells are labeled with tritiated thymidine ([^{3}H]dThd), mixed with unlabeled V79 cells, and centrifuged gently to form multicellular clusters about 1.6 mm in diameter. The short range of the ^{3}H β particles effectively allows only self-irradiation of labeled cells and no cross-irradiation of unlabeled cells. The percentage of labeled cells is controlled precisely by varying the number of labeled cells mixed with unlabeled cells prior to assembling the cluster. The clusters are assembled in the absence or presence of 100 μ*M* lindane, a chemical that is known to inhibit formation of gap junctions. After the clusters are maintained at 10.5°C for 72 h, the cells are dispersed and plated for colony formation. In the case of 100% labeling, the survival of cells in the cluster depends exponentially (SF = $e^{-A/1.8}$) on the cluster activity *A* (in kBq), and lindane has no effect on the response. A two-component exponential response is obtained for 50% labeling in the absence of lindane (SF = 0.33 $e^{-A/0.81}$ + 0.67 $e^{-A/11.8}$), and lindane has a marked effect on the response (SF = 0.33 $e^{-A/1.6}$ + 0.67 $e^{-A/41.6}$). These data suggest that bystander effects play an important role in the biological response of V79 cells when the ^{3}H is localized in the cell nucleus and distributed nonuniformly among the cells. In contrast, bystander effects cannot be detected above traditional radiation effects (i.e. direct + indirect) when the ^{3}H is localized in the cell nucleus and distributed uniformly among the cells. These results indicate that this multicellular cluster model is well suited for studying the effects of nonuniform distributions of radioactivity, including bystander and "hot-particle" effects. Furthermore, these results suggest that bystander effects may play an important role in the prediction of the biological effects of radiopharmaceuticals used in medical diagnosis and treatment. © 1999 by Radiation Research Society

INTRODUCTION

Over the past several years there have been several reports that cells that have received no radiation exposure suffer biological consequences when they are in the presence of cells that have been irradiated (*1–5*). This phenomenon has been termed the bystander effect. Nagasawa and Little (*1*) used acute external beams of α particles to irradiate monolayers of Chinese hamster ovary cells with low doses. These exposures led to the formation of sister chromatid exchanges in 30–50% of the cells despite the fact that statistically only about 1% of the cell nuclei could have been traversed by an α particle. They concluded that genetic damage can be imparted to "bystander" cells when cell populations are exposed to low doses from α particles. Similar observations were made by Deshpande *et al.* (*2*). Azzam *et al.* (*5*) studied the mechanisms of the bystander effect by showing that the expression levels of TP53, CDKN1A, CDC2, CCNB1 and RAD51 are significantly modulated when human diploid cell populations are irradiated with low doses of α particles where only a small fraction of the nuclei are actually hit. They also found that the extent of modulation was significantly reduced when lindane, an inhibitor of gap-junction intercellular communication (*6, 7*), was present during the irradiation period. These data suggest that gap-junction intercellular communication may play an important role in the bystander effect.

While the studies described above involve the use of α particles, Mothersill and Seymour (*4*) have irradiated cells with γ rays to study the bystander effect. In this case, the gap-junction inhibitor phorbol myristate acid actually increased killing by the bystander effect. Based on these data, they suggested that signal transduction mechanisms, as op-

[1] Author to whom correspondence and requests for reprints should be addressed.

posed to the release of a factor that is directly cytotoxic, may control death or survival due to the bystander effect.

The studies of Nagasawa and Little (*1*), Deshpande *et al.* (*2*) and Mothersill and Seymour (*4*) raise interesting points regarding the biological effects of ionizing radiation, in particular the bystander effect. As noted by these authors and others (*3, 8, 9*), the bystander effect is particularly relevant to the "hot-particle" problem as well as the biological effects of incorporated radionuclides in general. However, there remain several aspects to be addressed such as: (1) What is the significance of the bystander effect compared to the overall effect to the cell when it experiences damage from both bystander and traditional radiation effects (i.e. direct + indirect)? (2) Can bystander effects be observed in three-dimensional tissue models? (3) Do bystander effects indeed result from nonuniform distributions of radioactivity? (4) If so, what types of ionizing radiation produce significant bystander effects? The present work attempts to address some of these questions using a novel three-dimensional cell culture model and precisely controlled nonuniform distributions of incorporated radionuclides to deliver radiation exposures.

MATERIALS AND METHODS

Radiochemical and Quantification of Radioactivity

Tritiated thymidine ([^{3}H]dThd) was obtained from NEN Life Science Products (Boston, MA) as a sterile aqueous solution at a concentration of 37 MBq/ml and a specific activity of 3000 GBq/mmol. The activity of ^{3}H was measured with a Beckman LS3800 automatic liquid scintillation counter (Fullerton, CA) by transferring aliquots of radioactive culture medium into 6 ml of Aquasol® liquid scintillation cocktail (NEN Research Products, Boston, MA). The detection efficiency for the 5.7 keV β particles emitted by ^{3}H was 0.65. The radionuclide ^{3}H has a physical half-life of 12.3 years and emits β particles with a mean energy of 5.67 keV (*10*) corresponding to a mean range in water of about 1 μm (*11*).

Cell Line

Chinese hamster V79 lung fibroblasts (kindly provided by A. I. Kassis, Harvard Medical School, Boston, MA) were used in the present study, with clonogenic survival serving as the biological end point. V79 cells are known to exhibit some degree of gap-junction intercellular communication at 37°C (*12, 13*). The cells were cultured in minimum essential medium (MEM) supplemented with 10% heat-inactivated (57°C, 30 min) fetal calf serum with 2 m*M* L-glutamine, 50 U/ml penicillin and 50 μg/ml streptomycin (MEMA). The pH of the culture medium was adjusted to 7.0 with $NaHCO_3$. All media and supplements used in this study were from Life Technologies (Grand Island, NY). Cells were maintained in 175-cm^2 Falcon sterile tissue culture flasks (Becton Dickinson, Lincoln Park, NJ) at 37°C and 5% CO_2, 95% air, and were subcultured twice weekly or as required.

Radiolabeling and Assembly of Multicellular Clusters with 50% of Cells Labeled

V79 cells growing as monolayers in 175-cm^2 Falcon flasks were washed with 10 ml of phosphate-buffered saline, trypsinized with 0.05% trypsin–0.53 m*M* EDTA, and suspended at 2 × 10^6 cells/ml in calcium-free MEM with 10% heat-inactivated (57°C, 30 min) fetal calf serum, 2 m*M* L-glutamine, 50 U/ml penicillin and 50 μg/ml streptomycin (MEMB). Aliquots of 1 ml were placed in two sets of sterile 17 × 100-mm Falcon polypropylene round-bottom culture tubes (10 tubes in each set) and placed on a rocker-roller (Fisher Scientific, Springfield, NJ) for 3–4 h at 37°C in an atmosphere of 95% air and 5% CO_2. After this conditioning period, 1 ml of MEMB containing various activity concentrations (0–296 MBq) of [^{3}H]dThd was added to the first set of culture tubes containing 1 ml of V79 cells. Only 1 ml of MEMB was added to the other set of tubes. All tubes were then returned to the rocker-roller at 37°C, 95% air and 5% CO_2. After a 12-h period of labeling with radioactivity, the first set of tubes were removed and centrifuged at 2000 rpm at 4°C for 10 min. Aliquots of the supernatant were used to check the concentrations of radioactivity added. The cells were washed three times with 10 ml of MEM with 10% heat-inactivated (57°C, 30 min) calf serum, 2 m*M* L-glutamine, 50 U/ml penicillin and 50 μg/ml streptomycin (wash MEMA). The cells in the second set of tubes (unlabeled) were similarly washed and the contents of a given tube transferred to one of the first set of tubes containing radiolabeled cells. Finally, the pooled cells in each tube were suspended in 400 μl of MEMA or 0.58% DMSO (Sigma Chemical Co., St. Louis, MO) in MEMA or 0.58% DMSO–100 μ*M* lindane (hexachlorocyclohexane, γ-isomer from Sigma) and transferred directly to a sterile 400-μl polypropylene microcentrifuge tube with attached cap (Helena Plastics, San Rafael, CA) (Fig. 1). The concentration of lindane (i.e. 100 μ*M*) was selected based on a separate study as described below, and DMSO served as a control for lindane. The 400-μl tubes were centrifuged at 1000 rpm for 5 min at 4°C to form a multicellular cluster ~1.6 mm in diameter. The resulting clusters contained a total of 4 × 10^6 cells, of which 50% were labeled (Fig. 1). The capped

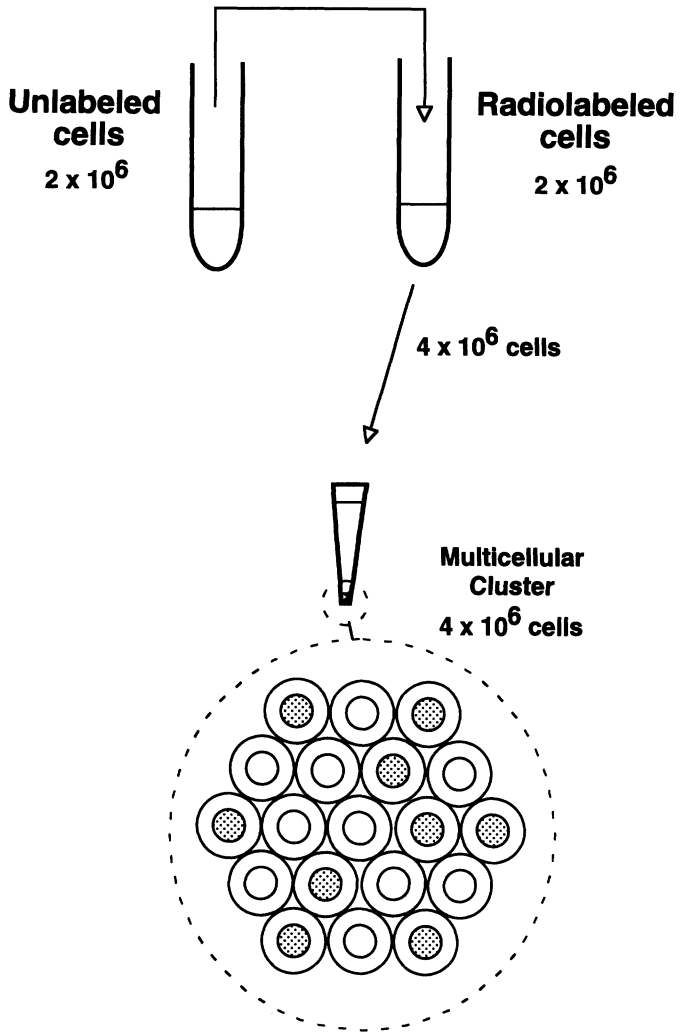

FIG. 1. Assembly of multicellular cluster of V79 cells in which 50% of the cells are radiolabeled with [^{3}H]dThd.

microcentrifuge tubes containing the clusters were placed in a perforated microcentrifuge tube rack and transferred to a refrigerator at 10.5°C. This temperature was selected because V79 cells can remain in the cluster configuration at this temperature for long periods (up to 72 h) without a decrease in plating efficiency. This was also true for V79 cells in suspension culture (*14*). Therefore, the cells accumulate the preponderance of their radioactive decays while in the cluster configuration as opposed to the radiolabeling and colony-forming periods. After 72 h at 10.5°C, the supernatant was carefully removed and the tube was vortexed to disperse the cell cluster. The cells were resuspended in MEMA, transferred to 17 × 100-mm Falcon polypropylene tubes, washed three times with 10 ml of wash MEMA, resuspended in 2 ml of MEMA, passed through a 21-gauge needle five times to disperse cells, and serially diluted (four 10× dilutions), and 1 ml of the appropriate dilutions (approximately 200 cells for control tubes) was seeded in triplicate into 60 × 15-mm Falcon tissue culture dishes. The dishes were then placed in an incubator at 37°C with 95% air and 5% CO_2. Aliquots were taken from each tube before serial dilution, and the mean radioactivity per cell was determined (*15*). The tissue culture dishes were removed from the incubator after 1 week, and the resulting colonies were washed 3 times with normal saline and 2 times with methanol and finally stained with 0.05% crystal violet. The colonies were counted under fluorescent light. A colony count of 25–250 was considered as a valid data point for each tissue culture dish. The surviving fraction compared to the parallel control was determined for each radioactivity concentration employed.

Chemotoxicity and Optimum Concentration of Lindane

Multicellular clusters were prepared wherein 50% of the cells were labeled with a fixed activity concentration of [^{3}H]dThd (148 MBq/ml) as described above. The clusters were maintained at 10.5°C for 72 h in the presence of 20–200 μ*M* of lindane. To achieve this, lindane was first dissolved in DMSO (5 mg/ml), filtered through a Millex®-HV filter (Millipore Corporation, Bedford, MA), and subsequently diluted with MEMA to a final concentration 20–200 μ*M* lindane, 0.58% DMSO. Parallel controls were established where clusters of unlabeled cells were maintained at the same concentrations of lindane with 0.58% DMSO. Thus, for each concentration of lindane, two tubes were prepared—one having a cluster of radiolabeled cells (50%) and one having a cluster of unlabeled cells. After 72 h the cluster was dismantled, the mean activity per cell was determined, and the cell survival was compared to that of its matched control using the procedure outlined above.

Assembly of Multicellular Clusters with 100% Radiolabeled Cells

Multicellular clusters in which 100% of the cells were radiolabeled were assembled using the cells prepared as above. In short, 1 ml of MEMB containing different concentrations of radioactivity was added to culture tubes containing 1 ml of conditioned cells (4 × 10^6 cells). Half of the concentrations used for the 50% labeling experiment were used to maintain approximately the same cluster activity. After an incubation period of 12 h at 37°C in an atmosphere of 95% air and 5% CO_2, the radiolabeled cells (4 × 10^6) were washed as above, suspended in 400 μl of MEMA, 0.58% DMSO in MEMA, or 0.58% DMSO–100 μ*M* lindane in MEMA, and transferred to a 400-μl microcentrifuge tube and centrifuged as described above. The microcentrifuge tubes containing the cell clusters were maintained at 10.5°C for 72 h, after which the surviving fraction of cells was determined as described above.

Response of Multicellular Clusters to Chronic and Acute Exposure to External γ Rays

Microcentrifuge tubes containing multicellular clusters prepared with 4 × 10^6 unlabeled cells as described above were transferred to a refrigerator at 10.5°C. The tubes were placed at different distances from a 370-MBq ^{137}Cs source housed in a small stainless steel capsule. Two control tubes were similarly maintained at 10.5°C without radiation exposure. The cumulated absorbed dose to the irradiated cells was measured using a Thomson-Nielson (Ottawa, Canada) miniature MOSFET dosimeter system. After 72 h of chronic irradiation, the cells were processed as described above to determine the surviving fraction. Cumulated doses of 2.4 to 12.7 Gy were delivered over 72 h at dose rates from 3 to 18 cGy/h, depending on the distance from the source. The response of the multicellular cluster to acute ^{137}Cs γ rays was also studied by maintaining identically prepared multicellular clusters at 10.5°C for 72 h and then irradiating them acutely at the same temperature in a J. L. Shepherd Mark I irradiator (San Fernando, CA). The acute dose rate was ~1–1.7 Gy per minute and total doses ranged from 1 to 12.5 Gy. After the acute irradiation, the cells were processed as above and the surviving fraction was determined compared to that for unirradiated control cells.

Gap-Junctional Intercellular Communication at 10.5°C

The scrape-loading and dye transfer technique of El-Fouly *et al.* (*12*) was used with slight modification. Approximately 4 × 10^6 cells were thawed from a stock of V79 cells maintained at −70°C, washed with MEMA, and immediately plated in a 30-mm Corning tissue culture dish (Corning, NY) with 2 ml of fresh MEMA. The dish was placed in an incubator at 37°C, 95% air and 5% CO_2 for 1 h and was then transferred to a refrigerator at 10.5°C. After 72 h, the confluent cell population was rinsed three times with Ca^{2+}-Mg^{2+}-free PBS. Two milliliters of PBS containing 0.05% Lucifer yellow (Molecular Probes, Inc., Eugene, OR) was added to the dish at room temperature and the monolayer was scraped along three parallel lines using a sterile scalpel blade. The dish was placed in the dark for 5 min to complete dye transfer. As Lucifer yellow is a hydrophilic fluorescent dye with a low molecular weight (mol. wt. 457.2), it can traverse gap junctions and therefore is an efficient means by which to monitor gap-junctional intercellular communication. The dye solution was decanted, the dish was rinsed three times with fresh PBS, and 2 ml of PBS was added to the dish. The plate was observed with an Olympus BX60 epifluorescence phase-contrast microscope illuminated with an Osram HBO 200 W lamp.

RESULTS

Response of Multicellular Clusters to External γ Rays

Figure 2 shows the dose–response curves for multicellular clusters of V79 cells exposed to chronic (3–18 cGy/h) and acute (1–1.7 Gy/min) ^{137}Cs γ irradiation. A least-squares fit of these data to the linear-quadratic model [$SF = \exp(-\alpha D - \beta D^2)$] yielded α(chronic) = 0.0440 ± 0.0183 Gy^{-1}, β(chronic) = 0.00391 ± 0.00231 Gy^{-2}, α(acute) = 0.118 ± 0.025 Gy^{-1}, and β(acute) = 0.00566 ± 0.0042 Gy^{-2}.

Response of Multicellular Clusters to [^{3}H]dThd

Figure 3 shows the surviving fraction of cells in the multicellular cluster as a function of the ^{3}H activity in the cluster when either 50% or 100% of the cells are radiolabeled. The response curve for 100% labeling is exponential, whereas the curve for 50% labeling is two-component exponential. A least-squares fit of these data to a two-component exponential function yields

$$SF = (1 - b)\, e^{-A/A_1} + b\, e^{-A/A_2}, \qquad (1)$$

where SF is the surviving fraction, A is the cluster activity, and b, A_1, and A_2 are the fitted parameters. For 50% labeling, the fitted parameters b, A_1, and A_2 are 0.67 ± 0.12, 0.81 ± 0.56 kBq, and 11.8 ± 3.1 kBq, respectively. In the

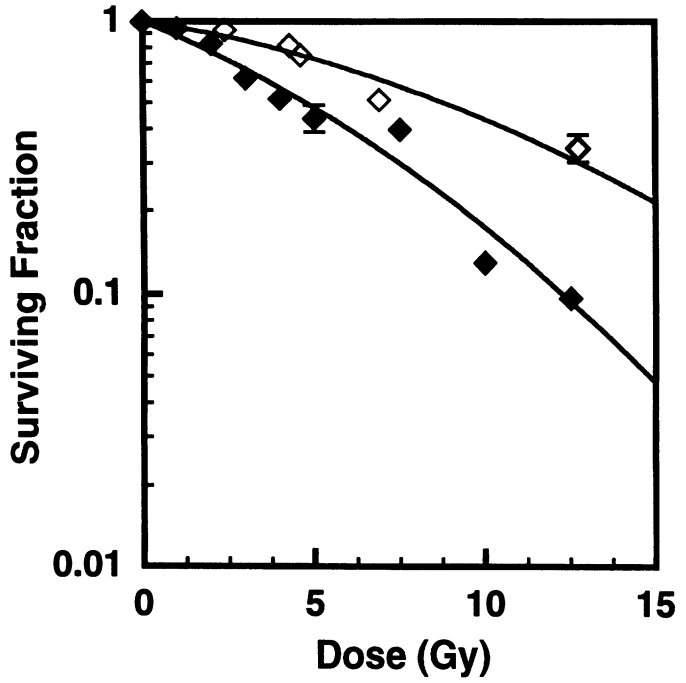

FIG. 2. Survival of V79 cells after acute (♦) and chronic (◊) irradiation of multicellular clusters with ^{137}Cs γ rays. Irradiations were carried out at 10.5°C. The acute dose rate was ~1–1.7 Gy per minute. For chronic irradiation, the tubes containing clusters were placed at different distances from a 370-MBq ^{137}Cs source housed in a small stainless steel capsule. After the acute and chronic irradiation, the clusters were dismantled, cells were processed, and the surviving fraction was determined compared to cells from unirradiated control clusters. Representative standard deviations are indicated by the error bars. Solid curves represent least-squares fits to the linear-quadratic model.

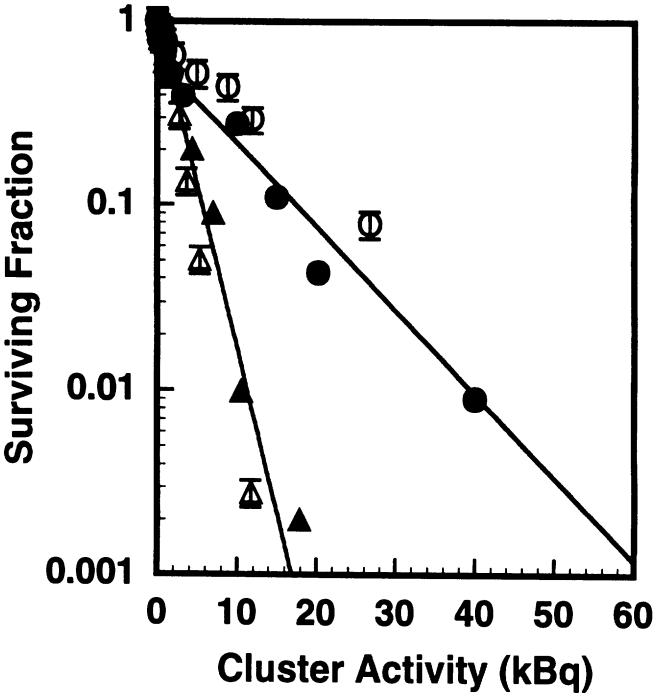

FIG. 3. Survival of V79 cells as a function of cluster activity of [^{3}H]dThd. Data are shown for experiments where 50% (●, ○) or 100% (▲, △) of the cells were radiolabeled in multicellular clusters which were maintained at 10.5°C for 72 h and then the surviving fraction was determined compared to unlabeled cells. Data from two independent experiments are plotted for each labeling condition and are differentiated by open and closed symbols. Representative standard deviations are indicated by the error bars.

case of 100% labeling, with $b = 0$, the fitted value of A_1 is 2.44 ± 0.11 kBq.

Chemotoxicity of Lindane

Figure 4 shows the fraction of surviving cells in multicellular clusters of V79 cells after a 72-h exposure to different concentrations of lindane in the culture medium. The surviving fraction compared to that for untreated controls remains close to unity up to about 100 μ*M* lindane, whereupon a significant decrease is observed. These data suggest that concentrations in excess of 100 μ*M* are not desirable for experiments involving inhibition of gap-junction intercellular communication due to associated cytotoxicity.

Optimum Concentration of Lindane to Inhibit Bystander Effect

Determination of the optimum concentration of lindane to minimize bystander effects is an essential element of the present study. Figure 5 shows the surviving fraction of V79 cells in multicellular clusters as a function of lindane concentration in the cell culture medium. In these experiments, 50% of the cells in the cluster are radiolabeled with approximately 4.8 mBq/cell of [^{3}H]dThd for a total cluster

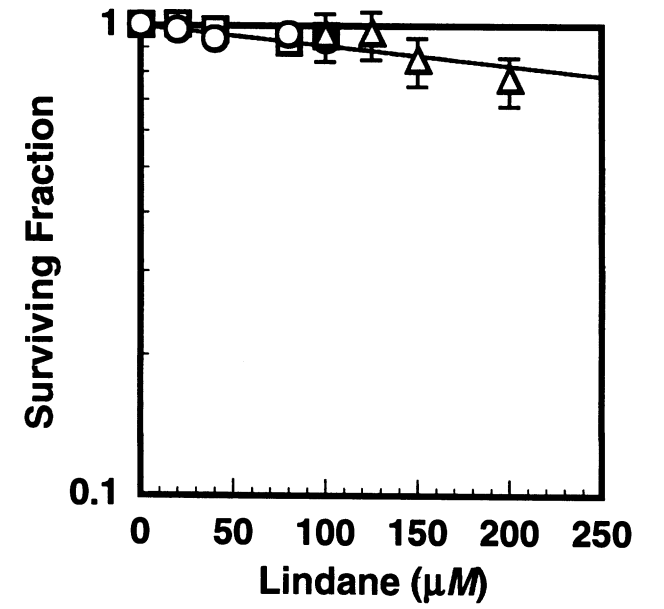

FIG. 4. Chemotoxicity of lindane when V79 multicellular clusters were exposed to the chemical at 10.5°C for 72 h. Representative standard deviations for individual data points are shown. Data from three independent experiments are indicated by different symbols (○, □, △).

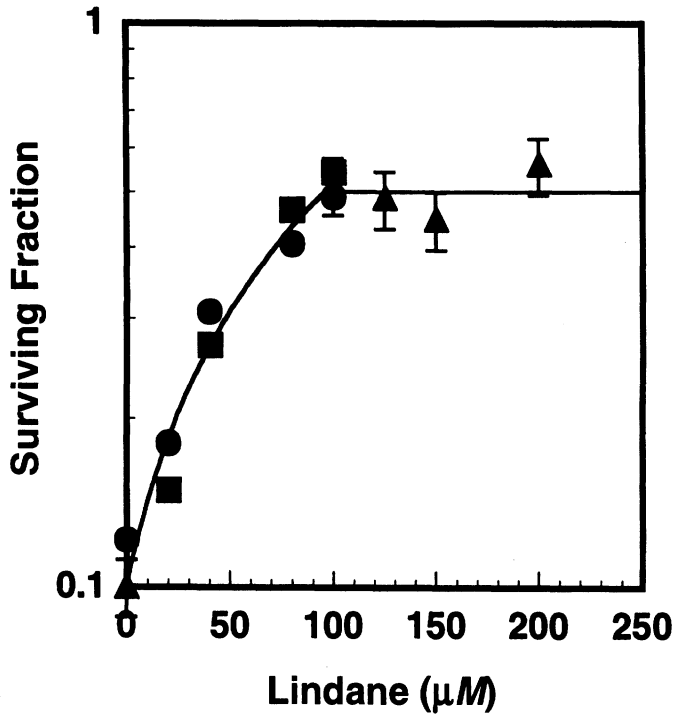

FIG. 5. Effect of lindane concentration on survival of V79 cells from multicellular clusters in which 50% of the cells are labeled with [^{3}H]dThd. The surviving fraction increased steadily with increasing lindane concentration up to 100 μ*M*, after which no additional protective effect was observed. Data from three independent experiments are indicated by three symbols (●, ■, ▲). Representative standard deviations are indicated by the error bars.

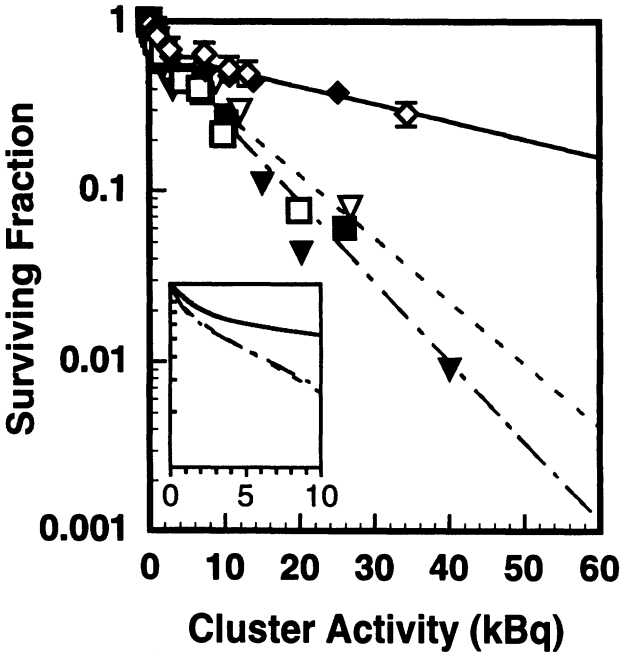

FIG. 6. Survival of V79 cells as a function of cluster activity of [^{3}H]dThd when 50% of the cells were labeled. Multicellular clusters were maintained at 10.5°C for 72 h in the presence of (1) [^{3}H]dThd (▼, ▽; data reproduced from Fig. 3); (2) [^{3}H]dThd + 0.58% DMSO (■, □); or (3) [^{3}H]dThd + 0.58% DMSO + 100 μ*M* lindane (◆, ◇). Data from two independent experiments are plotted for each treatment condition and are differentiated as open and closed symbols. Representative standard deviations are indicated by the error bars. The short-dashed, long-short dashed, and solid curves represent least-squares fits of the data to Eq. (1) for cases 1, 2 and 3, respectively.

activity of about 19 kBq. Multicellular clusters treated with neither [^{3}H]dThd nor lindane served as controls. The concentration of lindane in the culture medium has a marked impact on the surviving fraction of cells in the cluster, elevating the fraction from about 10% at 0 μ*M* lindane to about 50% at 100 μ*M* lindane for multicellular clusters with 50% labeled cells. No further significant increase in surviving fraction was observed at lindane concentrations in excess of 100 μ*M*. These data indicate that 100 μ*M* is the optimum concentration of lindane for carrying out detailed studies of bystander effects in V79 cell multicellular clusters.

Response of Multicellular Clusters to [^{3}H]dThd in the Absence and Presence of Lindane

Figure 6 shows the surviving fraction of cells in the multicellular cluster as a function of the ^{3}H activity in the cluster when only 50% of the cells are radiolabeled. In the absence of lindane, when the cluster activity increases, the surviving fraction decreases sharply to about 50% and then continues to decrease albeit with a more shallow slope. Essentially the same curve is obtained when these clusters are maintained in the presence of 0.58% DMSO. In contrast, clusters that were maintained in the presence of 0.58% DMSO + 100 μ*M* lindane show a similar sharp decrease in the slope of the response curve to about 50% survival and only limited cell killing at higher cluster activities. A least-squares fit of these data to Eq. (1) in the case of 100 μ*M* lindane gives values of 0.67 ± 0.03, 1.6 ± 0.3 and 41.6 ± 5.8 kBq for b, A_1 and A_2, respectively. The fitted parameters for the three irradiation conditions are summarized in Table 1.

The surviving fraction of cells in multicellular clusters assembled with 100% of the cells radiolabeled with [^{3}H]dThd is shown in Fig. 7 as a function of the cluster activity for the three experimental conditions: (1) [^{3}H]dThd, (2) [^{3}H]dThd + 0.58% DMSO, and (3) [^{3}H]dThd + 0.58% DMSO + 100 μ*M* lindane. The fraction of cells surviving compared to untreated controls was calculated in each case. The survival curves in all three cases are single-component exponential, which is commensurate with our earlier studies that examined the radiotoxicity of [^{3}H]dThd in V79 cells maintained in suspension culture (*14*). Least-squares fits of these data to Eq. (1) with $b = 0$ give A_1 values of 2.7 ± 0.1, 2.7 ± 0.2, and 2.8 ± 0.1 kBq for cases 1, 2 and 3, respectively. The fitted parameters for the three irradiation conditions are summarized in Table 1.

Evidence of Gap-Junctional Intercellular Communication at 10.5°C

To verify the capacity of V79 cells to form intercellular communication through gap junctions during maintenance

TABLE 1
Fitted Parameters for Survival Curves for Multicellular Clusters[a]

Treatment	Percentage cells labeled	b	A_1 (kBq)	A_2 (kBq)
[^{3}H]dThd[b]	100	0	2.7 ± 0.1	—
[^{3}H]dThd + 0.58% DMSO[b]	100	0	2.7 ± 0.2	—
[^{3}H]dThd + 0.58% DMSO + 100 μ*M* lindane[b]	100	0	2.8 ± 0.1	—
[^{3}H]dThd[c]	50	0.67 ± 0.12	0.81 ± 0.56	11.8 ± 3.1
[^{3}H]dThd + 0.58% DMSO[c]	50	0.75 ± 0.04	0.70 ± 0.17	9.3 ± 0.7
[^{3}H]dThd + 0.58% DMSO + 100 μ*M* lindane[c]	50	0.67 ± 0.03	1.6 ± 0.3	41.6 ± 5.8

[a] Standard errors are indicated.
[b] Least-squares fit to data in Fig. 7.
[c] Least-squares fit to data in Fig. 6.

at 10.5°C for 72 h, the transfer of Lucifer yellow dye between neighboring cells was studied in cells in monolayers. As shown in Fig. 8, Lucifer yellow was transferred into contiguous cells after the parallel lines were scraped in the monolayer with a scalpel. The highest intensity of Lucifer yellow was noticed in cells at the periphery of the scraped areas, and a gradient of decreasing intensity is evident as the dye spreads further into contiguous cells through gap junctions.

DISCUSSION

Radiopharmaceuticals are used widely in clinical medicine to diagnose and treat a variety of medical conditions. It is well known that when radiopharmaceuticals are administered to the patient, the radioactivity localizes in different tissues in the body and its distribution at the macroscopic and microscopic levels is nonuniform. The degree of nonuniformity can vary widely depending on a variety of factors. The biological consequences of nonuniform distributions of radioactivity in a given tissue can also vary substantially. Despite these well-known facts, current internationally accepted methods for assessing risks from diagnostic nuclear medicine procedures assume that the radioactivity is distributed uniformly in organs and tissues and that the biological response depends principally on absorbed dose, radiation type and tissue radiosensitivity (*16*). Bystander effects and other potential consequences of nonuniform distributions of radioactivity are ignored in these risk estimates. The same assumption is frequently made in assessing risks from environmental (e.g. ^{222}Rn) and accidental (e.g. ^{137}Cs, ^{131}I) exposures to radioactivity. Adelstein *et al.* (*17*) and Makrigiorgos *et al.* (*18*) have raised important concerns regarding the assumption of uniform distribution of radioactivity and their impact on risk estimates. However, one of the major stumbling blocks to predicting the biological response of tissues with nonuniform distributions of radioactivity has been the absence of experimental models that allow tight control over the distribution of the radioactivity.

Multicellular Model

The data in the present work have been obtained with a new three-dimensional tissue culture model that has been designed specifically to quantify the impact of nonuniform distributions of radioactivity in tissues on the biological effect of the incorporated radionuclides. It is demonstrated that multicellular clusters can be assembled by mixing suspensions of radiolabeled and nonradiolabeled cells to achieve a controlled degree of nonuniformity of radioactivity in an *in vitro* multicellular cluster model (Fig. 1). This

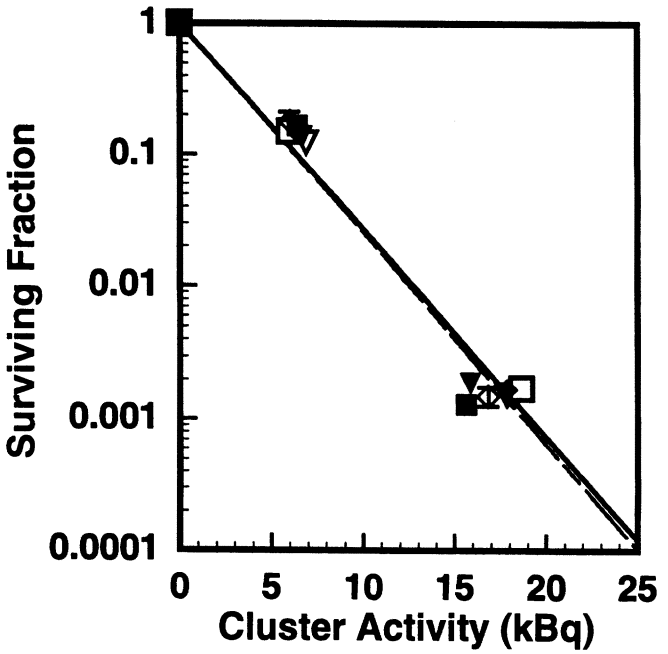

FIG. 7. Survival of V79 cells as a function of cluster activity of [^{3}H]dThd when 100% of the cells were labeled. Multicellular clusters were maintained at 10.5°C for 72 h in the presence of (1) [^{3}H]dThd (▼, ▽); (2) [^{3}H]dThd + 0.58% DMSO (■, □); (3) [^{3}H]dThd + 0.58% DMSO + 100 μ*M* lindane (◆, ◇). Data from two independent experiments are plotted for each treatment condition and are differentiated as open and closed symbols. Representative standard deviations are indicated by the error bars. The short-dashed, long-short dashed, and solid curves represent least-squares fits of the data to Eq. (1) for cases 1, 2 and 3 respectively.

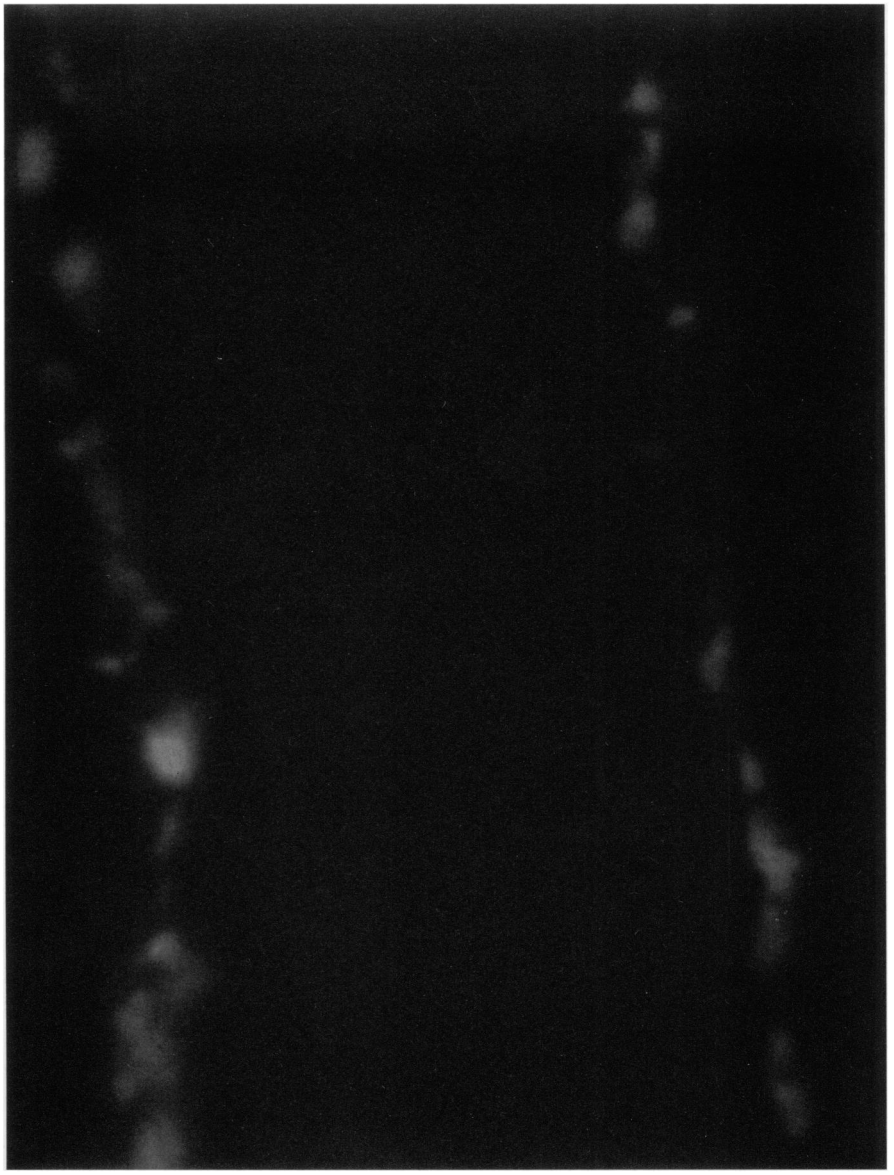

FIG. 8. Transfer of the fluorescent dye Lucifer yellow through gap junctions in V79 cells maintained as a monolayer culture at 10.5°C for 72 h.

new model affords a high degree of control over the percentage of radiolabeled cells in the cluster. The use of different radiochemicals can provide further control over the subcellular distribution of the radioactivity in the labeled cells. These degrees of control over the model are a major departure from past *in vitro* multicellular cluster models wherein multicellular spheroids are prepared prior to treatment with radioactivity, thus leading to a condition where only cells at the periphery of the cluster are effectively labeled (*19, 20*).

The response of the multicellular clusters used in the present work to external beams of ^{137}Cs γ rays is characterized in Fig. 2 for both acute and chronic irradiation. The dose–response curves with shoulders are characteristic of the response of mammalian cells to radiations of low linear energy transfer (LET). The acute doses were delivered at dose rates of 1–1.7 Gy/min, whereas the chronic irradiation was carried out at a dose rate of 3–18 cGy/h. The latter dose rates are more in keeping with those encountered in therapeutic nuclear medicine. Clearly, dose rate has a significant impact on the response.

The survival curves in Fig. 3 correspond to the case where V79 cells are labeled with [^{3}H]dThd. The dose responses for 50% and 100% labeling are markedly different from those observed when the cells are irradiated with external γ rays. In the case of 100% labeling of the cells in the cluster, the dose–response curve is exponential with a value of A_1 of 2.44 kBq. This exponential response is commensurate with the response of suspension cultures of V79 cells labeled with [^{3}H]dThd (*14*). In contrast, the dose–response curve for 50% labeling is two-component exponential, with the second component having a relatively

shallow slope compared to the first component as characterized by the parameters A_1 = 0.81 kBq and A_2 = 11.8 kBq. In other words, for a given amount of ^{3}H radioactivity in the cluster, the two labeling conditions (50%, 100%) yield very different surviving fractions. Therefore, the distribution of radioactivity in the cluster plays an important role in the biological response of the cells in the cluster. This is an important aspect of this new model that can be exploited to obtain quantitative data on the response of multicellular systems to nonuniform distributions of radioactivity.

Another significant feature of this new model is that typical cell survival experiments *in vitro* using radioprotectors or gap-junction inhibitors involve acute radiation exposures in the presence of chemotoxic concentrations of these agents. The cells are usually washed free of the agent immediately after the irradiation and plated for colony formation. When cells are irradiated by incorporated radionuclides, the radiation dose is delivered chronically. To examine the capacity of radioprotectors or gap-junction inhibitors to modify effects caused by chronic irradiation by incorporated radionuclides, the chemical agent should be present throughout the irradiation period (*21*). However, chronic exposure of cultured cells to these chemical agents at 37°C leads to extreme chemotoxicity, particularly when levels sufficient to afford protection are used (*21*). The results in Figs. 4 and 5 show that this problem can be overcome by maintaining the cells at 10.5°C. Under these conditions, the V79 cells did not divide and only minimal chemotoxicity was observed for both control and treated cells when the lindane concentration was maintained at or below 100 μM.

Chinese hamster V79 cells maintained at 37°C have been shown to exhibit intercellular communication through gap junctions. This has been demonstrated by freeze-fracture coupled with quantitative morphology (*13*) as well as the scrape-loading and dye transfer technique (*12*). However, to the best of our knowledge, the capacity of V79 cells to form gap junctions at 10.5°C has not been demonstrated. In the present study, this aspect has been explored by maintaining confluent monolayers of V79 cells at 10.5°C for 72 h and then studying the transfer of the fluorescent dye Lucifer yellow to detect gap-junctional intercellular communication. Figure 8 shows that V79 cells indeed retain their ability to form membrane channels through gap junctions even at 10.5°C, a process that can be seen efficiently through positive dye transfer into contiguous cells.

In view of the versatility and reproducibility of this new multicellular cluster model, it is possible that it may merit consideration for assessing bystander effects as set forth by Mill *et al.* (*8*) in their recent Letter to the Editor. Mill *et al.* (*8*) have argued that to clearly establish the existence of a bystander effect in the case of hot particles (and nonuniform activity distributions in general), "an internationally validated *in vitro* assay together with an internationally validated dosimetry protocol" is needed. The present experimental *in vitro* model, coupled with our theoretical multicellular dosimetry model (*22*), may be considered as a candidate for this purpose. It should be noted, however, that the current experimental protocol uses a maintenance temperature of 10.5°C, which may have an impact on metabolic processes such as DNA repair and cell proliferation. Ward *et al.*, (*23*) have shown that irradiated V79 cells are capable of repairing DNA single-strand breaks at temperatures as low as 10°C, albeit at a reduced rate. Double-strand breaks were not repaired at this temperature. However, despite the dependence of repair on temperature, a 3-h incubation of the irradiated cells at this temperature had no impact on cell survival. Nevertheless, the maintenance temperature in the present model can be increased to 37°C; this will reduce the capacity to introduce adequate concentrations of chemical modifiers such as DMSO and lindane without leading to undesired chemotoxicity.

The Bystander Effect

The β particles emitted by ^{3}H have a spectrum of energies from 0–18.6 keV (*10*) with corresponding ranges in water from 0–7 μm (*24*). The mean energy is only 5.7 keV, which corresponds to a range of only 1 μm in water (*24*). The mean diameter of a V79 cell is 10 μm and its nucleus has a mean diameter of 8 μm (*21*). Since the ^{3}H is incorporated into the DNA of the nuclei of labeled cells, the nuclei in these cells will be efficiently self-irradiated by the low-energy β particles emitted by the radionuclide. However, β particles emitted by ^{3}H decays in the cell nucleus must travel 2 μm (range of 10 keV electron, ref. *24*) just to get from the perimeter of the nucleus of a labeled cell to the perimeter of a nucleus of an unlabeled cell. The distance to the nucleus of the unlabeled cell is considered important because the nucleus presumably contains the primary radiosensitive targets. Since the electrons are emitted by decays occurring randomly throughout the nucleus, nearly all of the β particles will have to travel substantially more than 2 μm just to reach the nucleus of an unlabeled cell. Given that very few of the β particles emitted are in excess of the minimum requirement of 10 keV, the cross-dose received by cells in the cluster is negligible. This premise is supported by the multicellular dosimetry calculations of Goddu *et al.* (*22*) that show that cross-dose for electrons in this energy range is negligible when the radioactivity is localized in the cell nucleus. Therefore, in the absence of bystander effects, one anticipates essentially no killing of unlabeled cells, which should translate into a 50% surviving fraction in the case of 50% labeling at high cluster activities. The steep first component (A_1 = 0.81 kBq) of the two-component dose–response curve in Fig. 3 shows that about 50% of the cells are indeed killed. However, the second component (A_2 = 11.8 kBq) indicates that the unlabeled cells continue to be killed as the activity in the labeled cells is increased even though the unlabeled cells are not significantly irradiated. This suggests that a bystand-

er effect is responsible for the killing of unlabeled cells and, unlike the results of Mothersill and Seymour (*4*), the effect does not saturate with increasing dose (i.e. activity in the labeled cells).

To elucidate the potential mechanisms responsible for the bystander effect observed in Fig. 3, the gap-junction inhibitor lindane was added to the culture medium prior to formation of the multicellular clusters in which 50% of the cells were labeled. Figure 6 shows that 100 μM lindane has a marked impact on the survival of V79 cells with the value of A_2 in Eq. (1) changing from 11.8 kBq to 41.6 kBq. The solvent 0.58% DMSO had no impact on the response of the V79 cells. If the bystander effect blocking factor (BBF) is defined as the ratio

$$\text{BBF} = \frac{A_2 \text{ (with lindane)}}{A_2 \text{ (without lindane)}}, \qquad (2)$$

then the bystander effect blocking factor for 50% labeling of cells in the multicellular cluster with [^{3}H]dThd and maintenance in culture medium with 0.58% DMSO + 100 μM lindane is 3.5 $\pm$ 1.0. Since lindane is known to be a gap-junction inhibitor (*6, 7*), and it has been demonstrated in the present study that V79 cells form gap junctions at 10.5°C, it is likely that the bystander effects observed when 50% of the cells in the cluster are labeled with [^{3}H]dThd are due primarily to intercellular communication processes that depend on the formation of gap junctions which connect adjacent cells (*25*).

While lindane is known to be an inhibitor of gap-junction intercellular communication, it is also known to affect other processes that may pertain to its apparent ability to decrease bystander effects. For example, lindane may increase levels of superoxide dismutase and the extent of lipid peroxidation (*26, 27*) and cause alterations in intracellular free calcium and mitochondrial transmembrane potential (*28*). It may also increase the activity of NADPH-cytochrome P450 and the ratio of superoxide anion production/superoxide dismutase activity (*29*) and the formation of reactive oxygen species that result from the metabolism of lindane (*30*). Therefore, it is possible that mitigation of bystander effects by lindane may be due not only to inhibition of gap-junctional intercellular communication but also to these other processes.

Bystander Effects Relative to Conventional Radiation Effects

To assess the relative importance of bystander effects compared to conventional radiation effects (i.e. direct + indirect), the clusters were assembled such that 100% of the cells were again labeled with [^{3}H]dThd. Figure 7 shows the response of multicellular clusters treated with [^{3}H]dThd, [^{3}H]dThd + 0.58% DMSO, or [^{3}H]dThd + 0.58% DMSO + 100 μM lindane. The response of the V79 cells to the three treatment regimens is essentially the same within experimental uncertainties. Each of the cells in the cluster is surrounded by approximately 13 neighbors (*22*). Hence the biological effect imparted to a given target cell in the cluster is due not only to the ^{3}H decays that occur in the target cell but also to the sum of the bystander effects imparted by the neighboring cells. Therefore, since lindane had no impact on cell survival, the contribution of the bystander effect appears to be negligible for this biological end point in the case of 100% labeling, at least over the range of activities considered.

It thus stands to reason that the impact of the bystander effect on cell survival depends on the percentage of cells in the cluster that are labeled, with the effect being most pronounced at low labeling percentages and when cross-irradiation between cells is absent or minimal. Accordingly, it is anticipated that a somewhat smaller bystander effect may be observed when cells are labeled with radionuclides that emit particles with ranges of several cell diameters or more (e.g. ^{131}I) because cross-irradiation plays a more important role in these cases (*22*).

Finally, it should be noted that the arguments made above are based on cell survival data alone. While it is not expected that data based on other biological end points will point toward very different conclusions than those reached above, the importance of examining other end points is recognized.

ACKNOWLEDGMENTS

The authors would like to thank Prof. James E. Trosko, Michigan State University College of Human Medicine, for providing advice and his protocols for the scrape-loading and dye transfer technique. They are also grateful to Dr. Satam Banga, UMDNJ–New Jersey Medical School, for his assistance with the fluorescence microscopy techniques used in this work.

Received: March 31, 1999; accepted: May 6, 1999

REFERENCES

1. H. Nagasawa and J. B. Little, Induction of sister chromatid exchanges by extremely low doses of alpha-particles. *Cancer Res.* **52**, 6394–6396 (1992).
2. A. Deshpande, E. H. Goodwin, S. M. Bailey, B. L. Marrone and B. E. Lehnert, Alpha-particle-induced sister chromatid exchange in normal human lung fibroblasts—Evidence for an extranuclear target. *Radiat. Res.* **145**, 260–267 (1996).
3. M. Sigg, N. E. A. Crompton and W. Burkhart, Enhanced neoplastic transformation in an inhomogeneous radiation field: An effect of the presence of heavily damaged cells. *Radiat. Res.* **148**, 543–547 (1997).
4. C. Mothersill and C. B. Seymour, Cell–cell contact during γ irradiation is not required to induce a bystander effect in normal kidney keratinocytes: Evidence for release during irradiation of a signal controlling survival into the medium. *Radiat. Res.* **149**, 252–262 (1998).
5. E. I. Azzam, S. M. de Toledo, T. Gooding and J. B. Little, Intercellular communication is involved in the bystander regulation of gene expression in human cells exposed to very low fluences of alpha particles. *Radiat. Res.* **150**, 497–504 (1998).
6. X. Guan and R. J. Ruch, Gap junction endocytosis and lysosomal degradation of connexin43-P2 in WB-F344 rat liver epithelial cells treated with DDT and lindane. *Carcinogenesis* **17**, 1791–1798 (1996).
7. K. A. Criswell and R. Loch-Caruso, Lindane-induced elimination of

gap junctional communication in rat uterine monocytes is mediated by an arachidonic acid-sensitive cAMP-independent mechanism. *Toxicol. Appl. Pharmacol.* **135**, 127–138 (1995).

8. A. J. Mill, M. W. Charles and P. J. Darley, Enhanced neoplastic transformation in an inhomogeneous radiation field: An effect of the presence of heavily damaged cells. *Radiat. Res.* **149**, 649–651 (1998). [Letter to the Editor]
9. N. E. A. Crompton, M. Sigg and W. Burkart, Enhanced neoplastic transformation in an inhomogeneous radiation field: An effect of exposure to supralethally damaged cells. *Radiat. Res.* **149**, 651–653 (1998). [Letter to the Editor]
10. E. Browne and R. B. Firestone, *Table of Radioactive Isotopes.* Wiley, New York, 1986.
11. ICRU, *Photon, Electron, Proton and Neutron Interaction Data for Body Tissues.* Report 46, International Commission on Radiation Units and Measurements, Bethesda, MD, 1992.
12. M. H. El-Fouly, J. E. Trosko and C. C. Chang, Scrape-loading and dye transfer: A rapid and simple technique to study gap junctional intercellular communication. *Exp. Cell. Res.* **168**, 422–430 (1987).
13. S. B. Yancey, J. E. Edens, J. E. Trosko, C. C. Chang and J. P. Revel, Decreased incidence of gap junctions between Chinese hamster V-79 cells upon exposure to the tumor promoter 12-*o*-tetradecanoyl phorbol-13-acetate. *Exp. Cell Res.* **139**, 329–340 (1982).
14. R. W. Howell, S. M. Goddu, A. Bishayee and D. V. Rao, Radioprotection against lethal damage caused by chronic irradiation with radionuclides *in vitro*. *Radiat. Res.* **150**, 391–399 (1998).
15. A. I. Kassis and S. J. Adelstein, A rapid and reproducible method for the separation of cells from radioactive media. *J. Nucl. Med.* **21**, 88–90 (1980).
16. ICRP, *Radiation Dose to Patients from Radiopharmaceuticals.* Publication 53, International Commission on Radiological Protection, Pergamon Press, Oxford, 1987.
17. S. J. Adelstein, A. I. Kassis and K. S. R. Sastry, Cellular vs. organ approaches to dose estimates. In *Proceedings of Fourth International Radiopharmaceutical Dosimetry Symposium* (A. T. Schlafke-Stelson and E. E. Watson, Eds.), pp. 13–25. National Technical Information Service, Springfield, VA, 1986.
18. G. M. Makrigiorgos, S. J. Adelstein and A. I. Kassis, Cellular radiation dosimetry and its implications for estimation of radiation risks. Illustrative results with technetium-99m-labeled microspheres and macroaggregates. *J. Am. Med. Assoc.* **264**, 592–595 (1990).
19. V. K. Langmuir, J. K. McGann, F. Buchegger and R. M. Sutherland, The effect of antigen concentration, antibody valency and size, and tumor architecture on antibody binding in multicell spheroids. *Nucl. Med. Biol.* **18**, 753–764 (1991).
20. R. Sutherland, F. Buchegger, M. Schreyer, A. Vacca and J. P. Mach, Penetration and binding of radiolabeled anti-carcinoembryonic antigen monoclonal antibodies and their antigen binding fragments in human colon multicellular tumor spheroids. *Cancer Res.* **47**, 1627–1633 (1987).
21. R. W. Howell, D. V. Rao, D-Y. Hou, V. R. Narra and K. S. R. Sastry, The question of relative biological effectiveness and quality factor for Auger emitters incorporated into proliferating mammalian cells. *Radiat. Res.* **128**, 282–292 (1991).
22. S. M. Goddu, D. V. Rao and R. W. Howell, Multicellular dosimetry for micrometastases: Dependence of self-dose versus cross-dose to cell nuclei on type and energy of radiation and subcellular distribution of radionuclides. *J. Nucl. Med.* **35**, 521–530 (1994).
23. J. F. Ward, C. L. Limoli, P. M. Calabro-Jones and J. Aguilera, An examination of the repair saturation hypothesis for describing shouldered survival curves. *Radiat. Res.* **127**, 90–96 (1991).
24. ICRU, *Stopping Powers for Electrons and Positrons.* Report 37, International Commission on Radiation Units and Measurements, Bethesda, MD, 1984.
25. R. Bruzzone, T. W. White and D. A. Goodenough, The cellular internet: On-line with connexins. *Bioessays* **18**, 709–718 (1996).
26. B. C. Koner, B. D. Banerjee and A. Ray, Organochlorine pesticide-induced oxidative stress and immune suppression in rats. *Ind. J. Exp. Biol.* **36**, 395–398 (1998).
27. B. Descampiaux, J. M. Leroux, C. Peucelle and F. Erb, Assay of free-radical toxicity and antioxidant effect on the Hep 3B cell line: A test survey using lindane. *Cell Biol. Toxicol.* **12**, 19–28 (1996).
28. R. Rosa, E. Rodriguez-Farre and C. Sanfeliu, Cytotoxicity of hexachlorocyclohexane isomers and cyclodienes in primary cultures of cerebellar granule cells. *J. Pharmacol. Exp. Ther.* **278**, 163–169 (1996).
29. K. A. Simon Giavarotti, L. Rodrigues, T. Rodrigues, V. B. Junqueira and L. A. Videla, Liver microsomal parameters related to oxidative stress and antioxidant systems in hyperthyroid rats subjected to acute lindane treatment. *Free Radic. Res.* **29**, 35–42 (1998).
30. P. Perocco, A. Colacci, C. Del Ciello and S. Grilli, Cytotoxic and cell transforming effects of the insecticide, lindane (γ-hexachlorocyclohexane) on BALB/c 3T3 cells. *Res. Commun. Mol. Pathol. Pharmacol.* **89**, 329–339 (1995).